Synthesis and Characterization of Ethylene Vinyl Acetate/ Mg–Al Layered Double Hydroxide Nanocomposites

T. Kuila,[1] H. Acharya,[1] S. K. Srivastava,[1] A. K. Bhowmick[2]

[1]*Inorganic Materials and Nanocomposite Laboratory, Department of Chemistry, Indian Institute of Technology, Kharagpur 721302, India*
[2]*Rubber Technology Centre, Indian Institute Technology, Kharagpur 721302, India*

Received 18 August 2006; accepted 9 November 2006
DOI 10.1002/app.25840
Published online in Wiley InterScience (www.interscience.wiley.com).

ABSTRACT: Mg–Al layered double hydroxide (LDH)/ Ethylene vinyl acetate (EVA-28) nanocomposites were prepared through solution intercalation method using organically modified layered double hydroxide (DS-LDH). DS-LDH was made by the intercalation of sodium dodecyl sulfate (SDS) ion. The structure of DS-LDH and its nanocomposites with EVA-28 was determined by X-ray diffraction (XRD) and transmission electron microscope (TEM) analysis. XRD analysis shows that the original peak of DS-LDH shifted to lower 2θ range and supports the formation of intercalated nanocomposites while, TEM micrograph shows the presence of partially exfoliated LDH nanolayers in addition to orderly stacked LDH crystallites in the polymer matrix. The presence of LDH in the nanocomposites has been confirmed by Fourier transform infrared (FTIR) analysis. The mechanical properties show significant improvement for the nanocomposite with respect to neat EVA-28. Thermogravimetric (TGA) analysis shows that thermal stability of the nanocomposites is higher than that of EVA-28. © 2007 Wiley Periodicals, Inc. J Appl Polym Sci 104: 1845–1851, 2007

Key words: EVA-28; nanocomposites; morphology; TEM; mechanical properties; TGA

INTRODUCTION

Polymer/inorganic layered materials nanocomposite is a class of composite materials in which the inorganic phase dimension are in the order of nanometer range. The materials generally used for the nanocomposite preparation includes silicate clay minerals.[1,2] manganese oxides,[3] molybdenum sulfide,[4] layered phosphates,[5] and layered double hydroxides (LDHs).[6–8] Compared to the conventional composites, these nanocomposites have been recognized as one of the most promising materials because of enhanced mechanical properties, thermal stability, reduced gas permeability, and flame retardancy.[9–12] So far, majority of research work focus on polymer nanocomposites based on layered materials of natural origin, such as montmorillonite type of layered silicate compounds[1,2,14] whereas, LDH system has been less studied.[9–13] However, polymer/LDH nanocomposites become an emerging class of materials due to their wide application as stabilizer, medical materials, flame retardants, and so on.[8]

LDHs and smectite clay mineral both are layered materials having 1 : 1 brucite like structure and 1 : 2 TOT structure, respectively. The difference between these types of materials lies in their interlayer charge. LDHs consist of positively charged metal oxide/ hydroxide layers and the interlayer exchangeable anions.[11] The general composition of LDHs can be represented by the ideal formula $[M^{II}_{(1-x)}M^{III}_{x}(OH)_2]^{x+}A^{m-}_{x/m}.nH_2O$, where M^{2+} is divalent cation, such as Mg^{2+}, Zn^{2+}, etc., M^{3+} is trivalent cations, such as Al^{3+}, Cr^{3+}, etc.,[8] and A is an anion with valency m (like Cl^-, CO_3^{2-}, SO_4^{2-}, and NO_3^-, etc). The schematic structure of organo modified LDH is shown in Figure 1.

LDHs based polymer nanocomposites can be synthesized by four different methods, such as *in situ* polymerization, direct intercalation, restacking, and coprecipitation.[7,10] Depending on the filler distribution, polymer/LDH nanocomposites can be defined as (i) intercalated nanocomposite, where the LDHs layers are arranged regularly and stacked parallel to each other, (ii) exfoliated nanocomposite, where the layers are randomly distributed, and (iii) partially exfoliated nanocomposite, where the LDH layers are stacked parallel to each other in addition to some randomly dispersed layers throughout the polymer matrix.[11,15] Neat LDH material is not suitable for the intercalation of polymer chains because the interlayer gallery distance of LDH is too short (about 0.76 nm) to penetrate and is incompatible with the organic nonpolar polymer chains. To overcome these problems the interlayer anions of LDHs have been replaced by any long chain organic anion so that the interlayer region is compatible with polymer chain and the interlayer gallery distance increases suffi-

Correspondence to: S. K. Srivastava (sunit@chem.iitkgp.ernet.in).
Contract grant sponsor: CSIR, New Delhi.

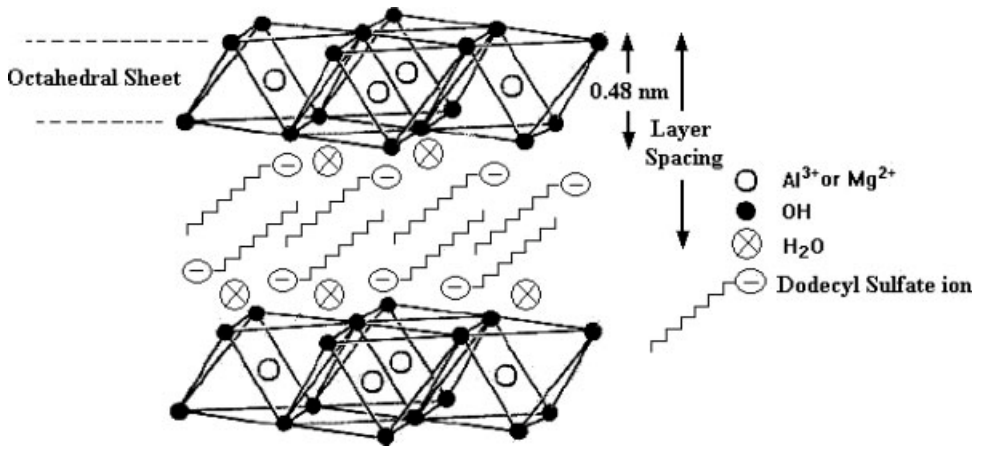

Figure 1 Crystallographic structure of DS-LDH.

ciently.[9,10] We have taken SDS as organic modifier and followed by *in situ* synthesis for the preparation of sodium dodecyl sulfate (SDS) intercalated LDH (DS-LDH).

Ethylene vinyl acetate copolymer (EVA) is available as different grades, such as rubber, thermoplastic elastomer, and plastic. Use of this copolymer is unlimited in different fields, such as electrical cable insulation, cable jacketing and repairing, water proofing, and packaging, etc. In the present article, we report the synthesis of Ethylene vinyl acetate (EVA) copolymer/Mg–Al LDH nanocomposites through solution intercalation method and investigate the effect of DS-LDH loading on EVA-28. The materials have been characterized by XRD, IR, SEM, and TEM analysis. The mechanical and thermal properties of the virgin EVA-28 and corresponding nanocomposites have been studied.

EXPERIMENTAL

Materials

EVA copolymer (Elvax 265) with melt flow index 3 g/10 min, density 955 kg/m^3 at 23°C, and vinyl acetate content of 28% w/w was received from DuPont (Chennai, India) and the crosslinking agent dicumyl peroxide (DiCUP-98, from Hercules, United States) was used to prepare the pristine EVA-28 and EVA-28/DS-LDH nanocomposites. $Mg(NO_3)_2 \cdot 6H_2O$ and $Al(NO_3)_3 \cdot 9H_2O$ were purchased from E. Merck, India. Sodium hydroxide (S.D.Fine chemicals, Boisar) and sodium dodecyl sulfate (SRL Pvt., Mumbai, India) were used as received. Toluene was purchased from SRL, Mumbai, India and was used without further purification.

Synthesis of organophilic LDH (DS-LDH)

DS-LDH was prepared by coprecipitation method. NaOH [0.8 g (0.02 mol)] was dissolved in 200 mL deionized water at room temperature followed by the addition of 6 g SDS. To this solution 19.65 g (0.075 mol) of $Mg(NO_3)_2 \cdot 6H_2O$ and 9.25 g (0.025 mol) of $Al(NO_3)_3 \cdot 9H_2O$ were added under flowing nitrogen gas. pH of the solution was maintained at 10 using 1*M* NaOH solution. After aging the resulting slurry at 75–80°C for 30 h, the precipitate was washed and dried at 60°C under vacuum for 72 h.

Synthesis of DS-LDH/EVA nanocomposites

In a 1-L Witts apparatus, EVA-28 was dissolved in dry toluene at 90°C. In another 100 mL round bottom flask DS-LDH was added to dry toluene and stirred for about 4 h to get a good dispersion. The appropriate amount of dispersed DS-LDH was added to EVA-28 solution under stirring at 90°C for 5 h. The crosslinking agent (Dicumyl peroxide) was then added to the mixture and the solvent was removed at reduced pressure. The nanocomposites so formed were compression-molded at 150°C for 45 min.

CHARACTERIZATION

X-ray diffraction (XRD) studies were carried out at room temperature on PAN analytical (PW 3040/60), model 'X' Pert Pro with Co K_α radiation (λ = 0.1790 nm). It was scanned from 2 to 10° with scanning speed of 3°/min. Fourier Transform Infrared spectrum was performed using Perkin–Elmer (FTIR Spectrometer RXI) over the wave number range 400–4000 cm^{-1}. The distribution of LDHs particles in the polymer matrix was studied with JEM 2100 JEOL, 200 KV transmission electron microscopes (TEM) with acceleration voltage of 100 kV and bright field illumination. Tensile properties of the virgin polymer and its nanocomposite were measured on a Zwick/Roell Z010 according to ASTM D-412 at a strain rate of 100 mm/min at (25 ± 2)°C. The standard deviation for tensile

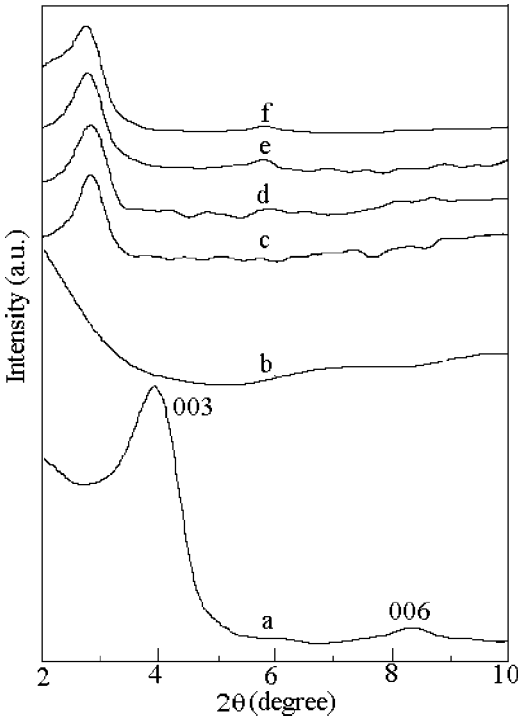

Figure 2 XRD spectra of (a) DS-LDH, (b) EVA-28, (c) EVA-28/DS-LDH (1 wt %), (d) EVA-28/DS-LDH (3 wt %), (e) EVA-28/DS-LDH (5 wt %), (f) EVA-28/DS-LDH (8 wt %).

strength and elongation at break were limits to ±5%. Scanning electron microscopic (SEM) photograph of tensile fracture specimen were carried out using JEOL (JSM-5800) with an acceleration voltage of 20 kV. Thermogravimetric analysis of neat EVA-28 and its nanocomposites (≈ 5.5 mg) were carried out on Redcroft 870 thermal analyzer, Perkin-Elmer with a heating rate of 10°C/min over a temperature range of 60–600°C in air atmosphere.

RESULTS AND DISCUSSION

XRD study

Figure 2 shows the XRD patterns at the range of $2\theta = 2$–10° for the DS-LDH, neat EVA-28 and EVA-28/LDH nanocomposites. The interlayer distance of DS-LDH and its composite with EVA-28 were calculated with the help of Bragg diffraction law. DS-LDH shows a sharp peak at $2\theta = 3.93^\circ$, corresponding to d_{003} peak with an interlayer distance of 2.61 nm, whereas the basal spacing of pristine LDH is 0.78 nm.[16] It is also reported that the individual dedecyl sulfate chain length and LDH sheet thickness are 2.07 and 0.48 nm respectively.[17,18] As a result the increase in basal spacing is due to the intercalation of dodecyl sulfate molecules between the hydrotalcite layers. In a case of nanocomposites containing 1, 3, 5, and 8 wt % of DS-LDH, the d_{003} peak of DS-LDH shifted to lower 2θ angles of ~2.7°, which indicates that the interlayer distance of DS-LDH further increases from 2.61 nm to 3.7 nm. It is worthy to note that the higher order (006) reflection peak at $2\theta = 8.4^\circ$ of DS-LDH weaken and shifted to $2\theta \approx 5.8^\circ$ for EVA-28/LDH nanocomposites. This observation suggests the formation of partially exfoliated LDH layers in addition to well ordered intercalated layers in the polymer matrix, which, in all probability is due to the loss of crystalline symmetry in the stacking direction of the hydroxide layers and lowering of number of hydroxide layers. Costa et al. also observed similar type of partially exfoliated structure for the polyethylene/Mg–Al LDH nanocomposite.[19]

Infrared analysis

Figure 3 shows the FTIR spectra of DS-LDH, EVA-28 and its nanocomposite containing 3 wt % DS-LDH. DS-LDH shows a presence of broad absorption band at 3400–3600 cm^{-1} due to OH stretching frequency. A peak due to bending vibration of interlayer water appears at about 1637 cm^{-1}. The peak around 1384 cm^{-1} is due to stretching mode of carbonate ion.[20] A broad absorption peak at about 3000 cm^{-1} is due to hydrogen bonded OH stretching of intercalated water molecules. The stretching vibration of C—H at 2851, 2920, and 2957 cm^{-1} and sulfate at 1217 cm^{-1} indicate the intercalation of SDS in LDHs layer. The bending mode vibration of interlayer anions appears around 1069 and 992 cm^{-1}. The

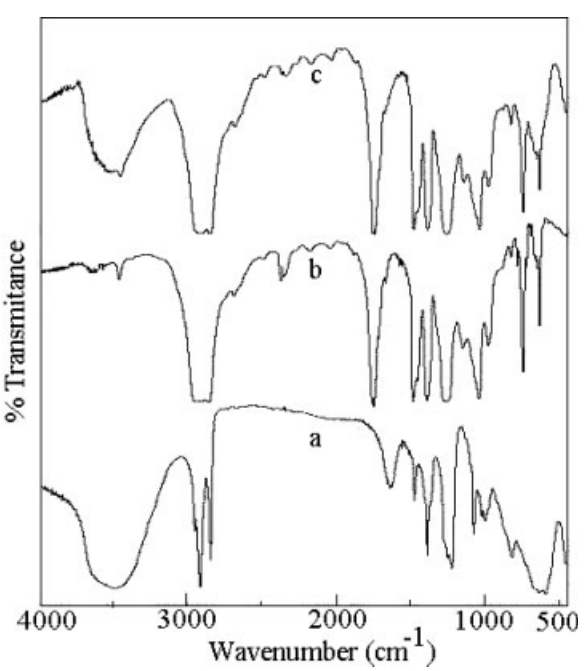

Figure 3 FTIR spectra of (a) DS-LDH, (b) EVA-28, (c) EVA-28/DS-LDH (3 wt %) nanocomposites.

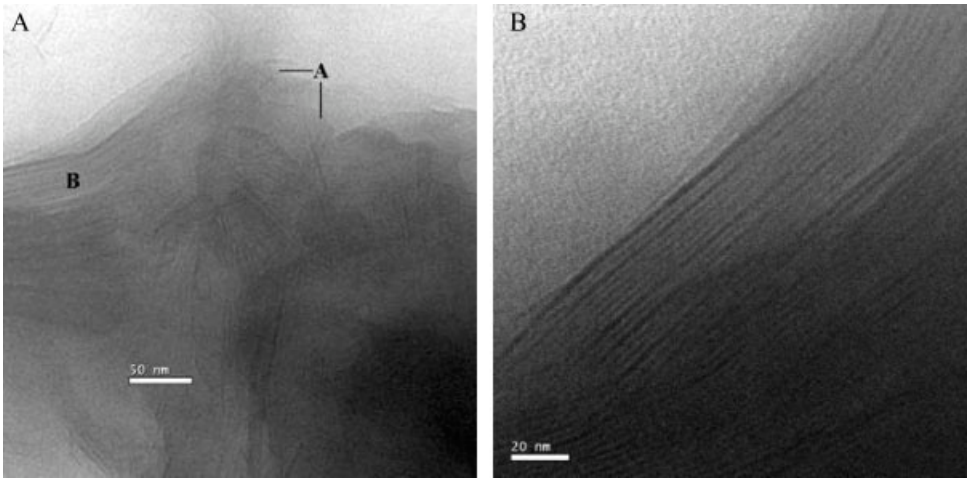

Figure 4 TEM images of EVA-28/DS-LDH (3 wt %) nanocomposite (A) at low magnification, (B) at high magnification.

bands recorded below 800 cm^{-1} are due to lattice vibration of M—O and O—M—O (M=Mg, Al) groups.[5] The IR spectra of EVA-28 and it composites with 3 wt % DS-LDH show characteristic bands of ester corresponding to C=O stretching around 1731 cm^{-1}. Appearance of some new peaks for EVA-28/DS-LDH nanocomposites at about 3500 cm^{-1} and the lattice vibration bands at 500–800 cm^{-1} region, which are absent in the case of EVA-28 provides an idea that the polymer chains are intercalated in the interlayer space of DS-LDH.

TEM analysis

Figure 4(A,B) shows TEM micrographs for nanocomposite containing 3 wt % DS-LDH. It is observed that the average lateral dimension of the DS-LDH layers varies from 50 to 150 nm and is homogeneously dispersed in the polymer matrix. In Figure 4(A) it is clearly observed that some of the LDH layers are partially exfoliated and marked as ''A'' whereas the major of DS-LDH layers are regularly oriented as shown by ''B.'' Figure 4(B) at higher magnification depicts that the nanocomposite mainly comprises of parallel DS-LDH nanolayers with interlayer spacing of 5–6 nm, which is much larger than that of DS-LDH itself. This is the direct evidence suggesting that the EVA-28 polymer chains are intercalated within the LDH layers, a fact which also supported by XRD as discussed earlier in Figure 2.

Mechanical properties

The effect of DS-LDH on the mechanical properties of EVA-28/DS-LDH has been studied and the results are presented in Figures 5 and 6. It is observed that the tensile strength (TS) and percent elongation at break (EB) for the nanocomposite containing 1 wt % DS-LDH compared to neat EVA-28 increases from 33 to 47 MPa (42% higher) and 877–924 (5% higher) respectively. The increase in tensile strength is likely due to the strong interfacial interaction between the hydroxyl group present in the DS-LDH and the polar acetate groups of EVA.[21] The intercalated rigid LDH layers efficiently transfers stress from LDH itself and enhance directly the stiffness in the nanocomposite as shown inset of Figure 6. The improvement in EB may be due to the orientation of the LDH platelet or chain slippage. A decreasing trend in TS as well as in EB is observed on further incorporation of LDH nanolayers in EVA. Such a drop in mechanical properties may be due to the increasing tendency of aggregation of LDH forming thereby some defects in the nanocomposites. Figure 5 shows the variation of tensile modulus at different percentage elongation. It can be noted that the tensile

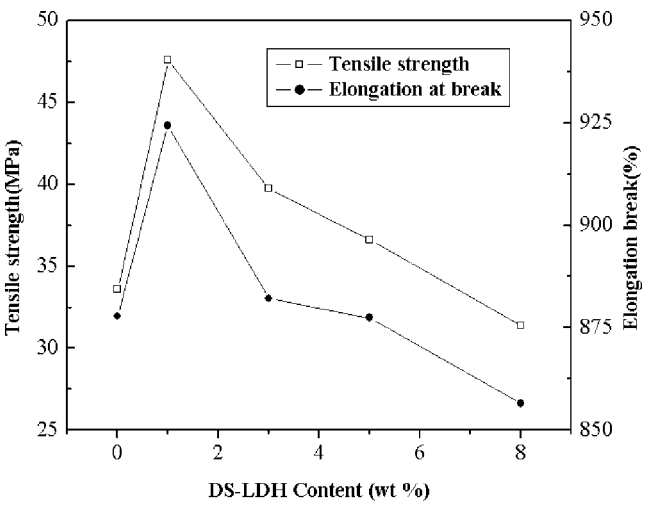

Figure 5 TS and EB of EVA-28/DS-LDH nanocomposites.

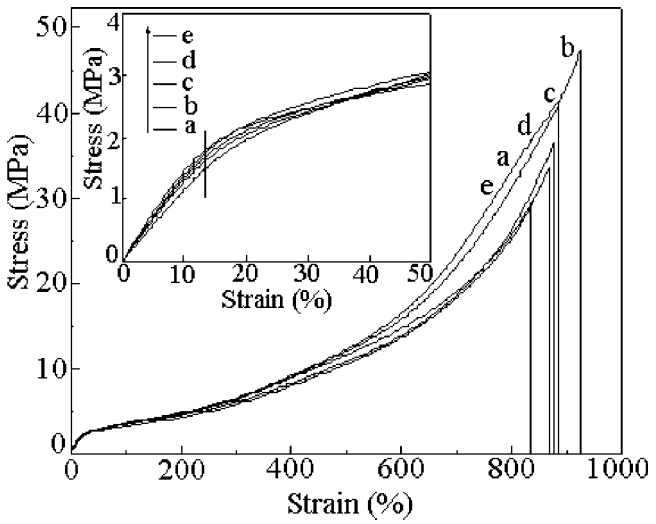

Figure 6 Stress versus strain plot of (a) EVA-28, (b) EVA-28/DS-LDH (1 wt %), (c) EVA-28/DS-LDH (3 wt %), (d) EVA-28/DS-LDH (5 wt %), (e) EVA-28/DS-LDH (8 wt %).

modulus for the nanocomposite containing 1 and 3 wt % DS-LDH is higher than the neat EVA. The enhanced tensile modulus of the nanocomposites is due to the formation of some shear zones when the nanocomposites are under stress and strain conditions.[15] Further, the addition of filler causes the reduction of modulus possibly due to the aggregation of DS-LDH nanolayers. In such cases, the crack growth occurs easily through filler agglomerates causing low strain failure.[22]

Fracture surface morphology

Figure 7 displays SEM micrographs taken from the tensile fracture surfaces of EVA-28 and its nanocomposites containing 1 wt % DS-LDH. The fractured surface image of neat EVA-28 clearly shows the presence of some cracks, while the nanocomposite containing 1 wt % DS-LDH does not show any prominent cracks. This is due to the formation of shear zones, which possibly reduces the formation of the cracks.[14] The strong interfacial interaction between the polymer matrix and DS-LDH forms some shear zones, which results in corresponding increase in TS of the nanocomposites. Moreover, it appears that the formation of micro-void around the LDH particles leads to the rough fracture surface which thereby favors the inter particle yielding and toughness of the nanocomposites and responsible for the improvements in mechanical properties.

TGA analysis

Figure 8 shows the thermograms of EVA-28 and the nanocomposites containing 1, 3, 5, and 8 wt % DS-LDH. It is evident that EVA-28 undergoes two-step decomposition[14]; the first step of degradation corresponds to the deacylation (225–412°C) while the second step associated with the polyethylene main chain decomposition (412–500°C). The figure clearly shows that the weight loss for the first step in all the nanocomposites is relatively more and may be attributed due to degradation of alkyl chains of organo-

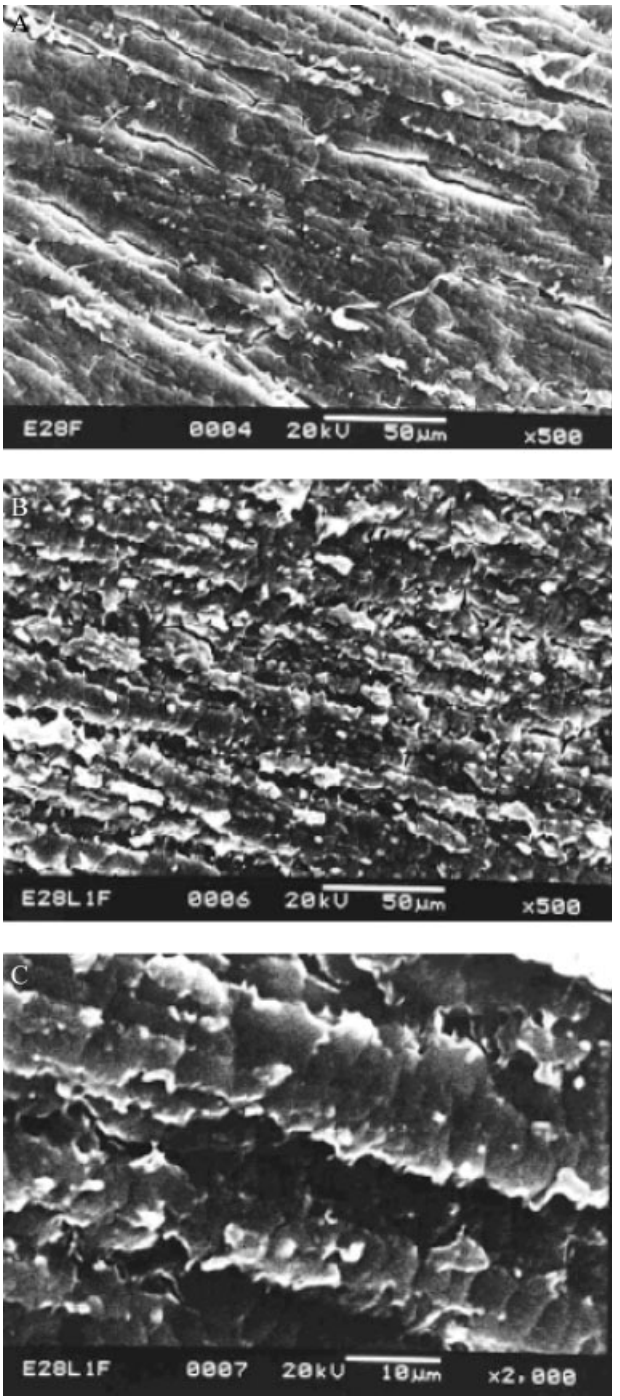

Figure 7 Tensile fracture surface morphology of (A) EVA-28, (B) EVA-28/DS-LDH (1 wt %) at low magnification, (C) EVA-28/DS-LDH (1 wt %) at high magnification.

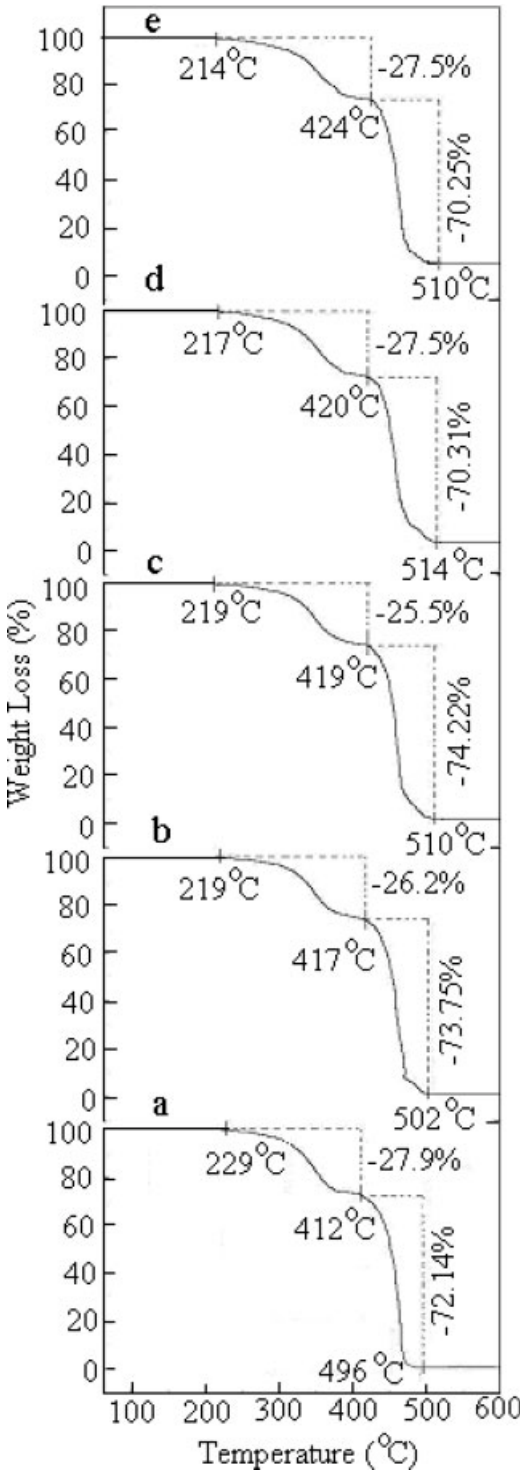

Figure 8 TGA curves of (a) EVA-28, (b) EVA-28/DS-LDH (1 wt %), (c) EVA-8/DS-LDH (3 wt %), (d) EVA-28/DS-LDH (5 wt %), (e) EVA-28/DS-LDH (8 wt %).

modified LDH.[7] Such an initial weight loss is anticipated to reinforce the charring process and could be more useful for the fire safety of nanocomposites. According to Chen and Qu[6] an efficient charring process in a flame retardant polymer occurs at a temperature higher than its processing temperature but much lower than its decomposition temperature. It is also observed that the first step weight loss for EVA-28/DS-LDH nanocomposites up to 3 wt % of LDH loading decreases than the neat EVA-28. This improvement in thermal stability is possibly due to the barrier effect of the homogeneously dispersed LDH layers, which inhibit the cooperative motion of small molecules during decomposition. However, EVA-28/DS-LDH nanocomposites containing higher LDH content exhibit no further improvement in first step decomposition process. This is possibly due to aggregation tendency of LDH layers in the EVA-28 matrix. The weight loss of EVA-28/LDH nanocomposites upto 3 wt % LDH content in the second step also increases with increasing final decomposition temperature. Therefore, such a weight loss at the second step of decomposition process is highly advantageous to promote the charring process and enhance the fire safety of nanocomposites.[6] Further, addition of LDH in EVA leads to the decrease in weight loss due to aggregation of LDH nanolayers that could form heat source domains in the degradation step.

CONCLUSIONS

EVA/DS-LDH nanocomposites synthesized by solution blending shows enhanced physicochemical properties. XRD analysis provides an idea that the polymer matrix is intercalated in between the LDH layers. TEM analysis shows that the LDH particles are well dispersed in the polymer matrix and confirms the formation of partially exfoliated nanocomposites. Mechanical properties of the nanocomposites are higher than the virgin polymer at low filler loading but at higher filler loading (8 wt %) tensile modulus decreases due to the aggregation of LDH layers, which is clearly observed by SEM analysis. Thermogravimetric analysis shows that the thermal stability of the nanocomposites is relatively higher and can be used as fire safety materials.

References

1. Ray, S. S.; Okamoto, M. Prog Polym Sci 2003, 28, 1539.
2. Srivastava, S. K.; Pramanik, M.; Acharya, H. J Polym Sci Part B: Polym Phys 2006, 44, 471.
3. Liu, Z. H.; Yang, X. J.; Makita, Y.; Ooi, K. Chem Lett 2002, 7, 680.
4. Heising, J.; Kanatzidis, M. G. J Am Chem Soc 1999, 121, 638.
5. Nakato, T.; Furumi, Y.; Terao, N.; Okuhara, T. J Mater Chem 2000, 10, 737.
6. Chen, W.; Qu, B. Chem Mater 2003, 15, 3208.
7. Chen, W.; Feng, L.; Qu, B. Chem Mater 2004, 16, 368.
8. Leroux, F.; Besse, J. P. Chem Mater 2001, 13, 3507.
9. Du, L.; Qu, B.; Meng, Y.; Zhu, Q. Compos Sci Technol 2006, 66, 913.

10. Hsueh, H. B.; Chen, C. Y. Polymer 2003, 44, 1151.
11. Costa, F. C.; Abdel-Goad, M.; Wagenknecht, U.; Heinrich, G. Polymer 2005, 46, 4447.
12. Costantino, U.; Gallipoli, A.; Nocchetti, M.; Camino, G.; Bellucci, F.; Frache, A. Polym Degrad Stab 2005, 90, 586.
13. Acharya, H.; Srivastava, S. K.; Bhowmick, A. K. Nanoscale Res Lett, 2007, to appear.
14. Pramanik, M.; Srivastava, S. K.; Samantaray, B. K.; Bhowmick, A. K. J Polym Sci Part B: Polym Phys 2002, 40, 2065.
15. Acharya, H.; Pramanik, M.; Srivastava, S. K.; Bhowmick, A. K. J Appl Polym Sci 2004, 93, 2429.
16. Chibwe, K.; Jones, W. Chem Commun 1989, 926.
17. Sundell, S. Acta Chem Scand A 1971, 31, 799.
18. Wilson, O. C.; Olorunyolemi, T.; Jaworski, A.; Borun, L.; Siriwat, A.; Dickens, E.; Oriakhi, C.; Lerner, M. Appl Clay Sci 1999, 15, 265.
19. Costa, F. R.; Satapathy, B. K.; Wagenknecht, U.; Weidisch, R.; Heinrich, G. Eur Polym J 2006, 43, 2140.
20. Lin, Y.; Wang, J.; Evans, D. G.; Li, D. J. Phys Chem Solids 2006, 67, 998.
21. Peeterbroeck, S.; Alexander, M.; Jerome, R.; Dobois, Ph. Polym Degrad Stab 2005, 90, 288.
22. Haworth, B.; Raymond, C. L.; Sutherland, I. Polym Eng Sci 2001, 41, 1345.